doi:10.1016/j.jmb.2007.09.018 J. Mol. Biol. (2007) 374, 791–805

JMB

Available online at www.sciencedirect.com

ScienceDirect

ELSEVIER

Multiple Tryptophan Probes Reveal that Ubiquitin Folds *via* a Late Misfolded Intermediate

Alexis Vallée-Bélisle and Stephen W. Michnick*

Département de biochimie
Université de Montréal
CP 6128, Station Centre-Ville
Montréal, Québec, Canada
H3C 3J7

Received 19 June 2007;
received in revised form
22 August 2007;
accepted 6 September 2007
Available online
12 September 2007

Much of our understanding of protein folding mechanisms is derived from experiments using intrinsic fluorescence of natural or genetically inserted tryptophan (Trp) residues to monitor protein refolding and site-directed mutagenesis to determine the energetic role of amino acids in the native (N), intermediate (I) or transition (T) states. However, this strategy has limited use to study complex folding reactions because a single fluorescence probe may not detect all low-energy folding intermediates. To overcome this limitation, we suggest that protein refolding should be monitored with different solvent-exposed Trp probes. Here, we demonstrate the utility of this approach by investigating the controversial folding mechanism of ubiquitin (Ub) using Trp probes located at residue positions 1, 28, 45, 57, and 66. We first show that these Trp are structurally sensitive and minimally perturbing fluorescent probes for monitoring folding/unfolding of the protein. Using a conventional stopped-flow instrument, we show that ANS and Trp fluorescence detect two distinct transitions during the refolding of all five Trp mutants at low concentrations of denaturant: T_1, a denaturant-dependent transition and T_2, a slower transition, largely denaturant-independent. Surprisingly, some Trp mutants (Ub^{M1W}, Ub^{S57W}) display Trp fluorescence changes during T_1 that are distinct from the expected U→N transition suggesting that the denaturant-dependent refolding transition of Ub is not a U→N transition but represents the formation of a structurally distinct I-state (U→I). Alternatively, this U→I transition could be also clearly distinguished by using a combination of two Trp mutations $Ub^{F45W\text{-}T66W}$ for which the two Trp probes that display fluorescence changes of opposite sign during T_1 and T_2 ($Ub^{F45W\text{-}T66W}$). Global fitting of the folding/unfolding kinetic parameters and additional folding-unfolding double-jump experiments performed on Ub^{M1W}, a mutant with enhanced fluorescence in the I-state, demonstrate that the I-state is stable, compact, misfolded, and on-pathway. These results illustrate how transient low-energy I-states can be characterized efficiently in complex refolding reactions using multiple Trp probes.

Keywords: ubiquitin; sequential *versus* parallel protein-folding mechanism; early and late low-energy intermediates; on-pathway versus off-pathway intermediates; tryptophan fluorescence probe

Edited by F. Schmid

Introduction

In the last decade, the general determinants of protein folding rate and mechanism have started to emerge from the comparison of numerous experimental studies on small proteins that fold without the accumulation of intermediate (I) states.[1–5] In contrast, studies on proteins that fold through one or more populated I-states have frequently resulted in controversies,[6] due mainly to the low structural

*Corresponding author. E-mail address: stephen.michnick@umontreal.ca.

Abbreviations used: Ub, mammalian ubiquitin; GdnHCl, guanidine hydrochloride; T, transition; I, intermediate; N, native; U, unfolded; A, amplitude; *F*, fluorescence; ANS, 8-anilino-1-naphtalenesulfonate.

resolution of the probes that are commonly used to monitor fast folding reactions. For example, tryptophan (Trp) or 8-anilino-1-naphtalenesulfonate (ANS) fluorescence spectroscopy, circular dichroism (CD) and absorbance spectroscopy cannot be used to assess whether additional folding transitions detected during protein refolding are due to non-obligatory transitions that often accompany "two-state" folding proteins (for example: proline *cis*-trapped unfolded molecules,[7] non-prolyl *cis*-trapped unfolded molecules,[8] small fraction slower folding proteins[9–12]), or are related to the presence of sequential I-states in a three-state mechanism.[13,14] A case in point is long-standing debates on the mechanisms of folding of the model protein ubiquitin (Ub), which have clearly highlighted this limitation over the years.[15–21] For example, various analyses of Ub refolding using the fluorescence of the genetically inserted Trp45 (Ub^{F45W}) to probe structure formation led to the proposals that this protein could fold either *via* an early hydrophobic intermediate,[15,16,21,22] an apparent two-state mechanism,[17,18,23,24] parallel folding pathways,[21] or through formation of some protein aggregates (Figure 1).[19] These ambiguities are not likely resolvable by using other spectroscopic techniques, since structural changes in small proteins do not often provide sufficient CD or absorbance signal changes to allow for efficient detection, and the ANS probe, despite its high sensitivity, may alter protein folding kinetics.[14,25] Alternative approaches using NMR spectroscopy to provide site-specific information on I-states have been developed and exploited with great success. On the other hand, equilibrium deuterium/hydrogen exchange experiments cannot determine whether the I-state is on-pathway,[26,27] pulse deuterium/hydrogen-exchange experiments are quite difficult to perform quantitatively,[28,29] and relaxation dispersion NMR experiments[30] necessitate that at least 0.5% of the I-state population is observable at equilibrium. Our ability to characterize complex refolding reactions would therefore be greatly improved if we could: (1) efficiently detect all the transient low-energy I-states that accumulate during protein folding; and (2) characterize the structural nature of the different transitions that are detected during a refolding kinetic experiment.

Here, we show that we can meet these criteria by monitoring protein refolding using the intrinsic fluorescence of several Trp mutants in which the inserted Trp substitute residues whose side-chains are solvent-exposed on the surface of the protein. Previous examples in the literature of Trp substitution as probes of folding or unfolding were done by conservative mutations of partially or completely buried aromatic residues to Trp or *vice versa*.[15,31–36] The strategy described here is more flexible, in that the Trp substitution can be made anywhere on the surface, allowing structural transitions in any region of the protein to be probed with high efficiency, with minimal or no apparent perturbation of refolding pathways. Specifically, we use different Trp probes in order to discriminate between folding transitions that represent conformational changes that occur in the entire protein population *versus* those that correspond to parallel folding pathways (Figure 1). For example, the relative folding amplitude of two transitions representing parallel pathways should remain relatively constant regardless of the probe used, since the amplitude of these transitions reflects mostly the fraction of molecules going through each path (Figure 1: two-state mechanism with parallel pathways).[14] On the other hand, one should expect that some Trp probes manifest refolding amplitudes that are distinct from the U→N fluorescence change for transitions that represent the formation and/or rearrangement of a structurally distinct I-state (Figure 1: three-state mechanism with sequential I-state. Trp fluorescence should display different sensitivity to T_1 and T_2, depending on whether it is located in the protein at position A or B).

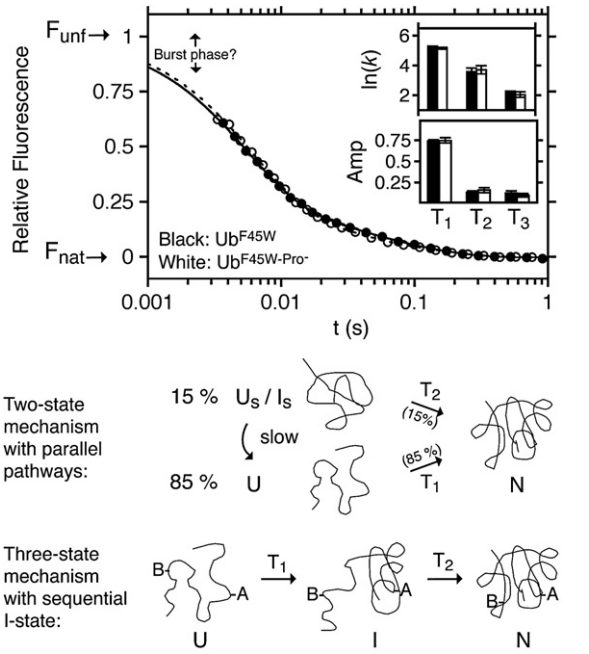

Figure 1. Ub refolding probed by Trp45 fluorescence. Refolding traces of Ub^{F45W} (filled symbols) and its proline-less mutant (open symbols) are better modeled with the sum of three exponential functions between 3.2 ms and 1 s at 0.45 M GdnHCl. Amplitudes and rate constants of the different transitions (T) are shown insert. It has been demonstrated that T_1 displays the characteristics of an apparent two-state transition,[17] and rapid unfolding-folding experiments[18,21] suggest that T_3 represents a small population of slow-folding proteins likely attributable to non-prolyl *cis*-trapped polypeptide.[8] T_2 could either represent a parallel channel involving around 15% of slower folding proteins (U_S or I_S: two-state mechanism with parallel pathways) or the structural rearrangement of a sequential I-state (three-state mechanism with sequential I-state). In this latter case, T_1 and T_2 should display very different refolding amplitudes depending on the probe location on the protein (ex: location A or B). The presence of a faster folding transition, inferred from a burst phase, is also the subject of debate.[17,18,20,21]

We apply our strategy to analyze the controversial refolding mechanism of the small ββαββαβ mammalian Ub (Figure 2(a)), a 76 amino acid residue protein that contains no natural Trp, no disulfide bond and possesses three proline residues in the *trans* conformation in the N-state.[37] Recently, Krantz *et al.*[17] demonstrated that the rate constant of the main refolding transition of Ub^{F45W}, T_1, displays the characteristics of an apparent two-state transition in the absence of a burst phase. Since then, this denaturant-dependent transition has been characterized extensively using both Φ and Ψ-value analysis.[23,24,40] However, Searle and colleagues demonstrated recently that two additional minor slower folding transitions, T_2 and T_3, are detected in a proline-less mutant form of Ub, suggesting that these transitions cannot be attributed to rate-limiting *cis-trans* prolyl isomerization events (Figure 1).[21] Rapid unfolding-folding experiments performed by us[18] and by Crespo *et al.*[21] suggest that T_3 represents a small population of slow-folding proteins likely attributable to non-prolyl *cis*-trapped polypeptide,[8] but the nature of T_2 is unknown. In the present work, Ub refolding was monitored using five different Trp probes in order to characterize both T_1 and T_2, the first and second folding transitions detected when a conventional stopped-flow instrument is used to trigger refolding. Surprisingly, we found that some single Trp mutants displayed refolding amplitude during T_1 that are distinct from the expected U→N fluorescence. This suggests that T_1, the denaturant-dependent folding transition, leads Ub to a structurally distinct I-state that rearranges in the N-state only through T_2, a second rate-limiting step. Global fitting analysis of the rate constants and amplitudes of T_1 and T_2, and additional folding-unfolding double-jump experiments performed with the help of an I-state-sensitive Trp probe allowed us to determine the stability, level of compaction and on-pathway nature of the late I-state. In addition, three out of the five Trp probes studied displayed a significant burst phase during Ub refolding at low concentrations of denaturant, providing further evidence for accumulation of early species within the dead time of our stopped-flow instrument (<3.2 ms).[20] The approach described here demonstrates how several solvent-exposed Trp probes can provide unambiguous evidence to characterize the different transitions detected during protein refolding with minimal perturbation of the protein folding landscape.

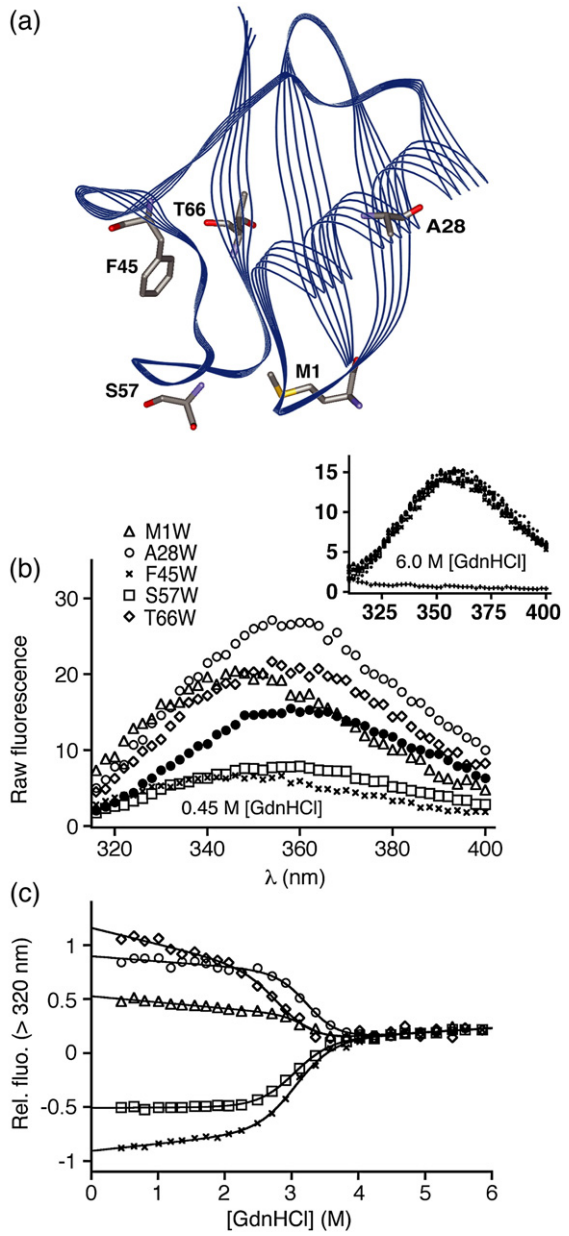

Figure 2. Equilibrium characterization of the single Trp mutants. (a) Ribbon representation of Ub structure. Amino acids with displayed side-chains are mutated to Trp in the present study (PDB code 1UBI[38]). (b) Fluorescence spectra of the Trp mutants in 0.45 M and 6.0 M GdnHCl (inset). Filled circles represent the fluorescence spectrum of an equimolar solution of *N*-acetyl-tryptophanamide (10 μM). Wild-type Ub (+) showed no significant intrinsic fluorescence when compared with the other single Trp mutants (inset). (c) Equilibrium stability curves of the different Trp mutants monitored using Trp fluorescence intensity (320 nm cut-off filter). Extrapolated free energies of unfolding in water (ΔG^{H_2O}) and their denaturant dependence (*m*-value) obtained from the best fits are reported in Table 1.

Results

The folding landscape of Ub is unaffected by Trp substitutions at solvent-exposed positions

We have created single Trp mutants at different residues whose side-chains are solvent-exposed in the native structure, in order to probe both the local and global structures of Ub with minimal perturbation. In the present study, amino acid residues Met1 (first hairpin), Ala28 (α-helix), Phe45 (original Trp location used to study the folding of Ub[15]), Ser 37 (3_{10} helix) and Thr66 (fifth β-strand) were chosen in

order to monitor the formation of different secondary structure elements of the protein (Figure 2(a)). In strong denaturing conditions (6.0 M guanidine hydrochloride (GdnHCl)), the fluorescence spectra of all single Trp mutants were found to be similar to an equimolar solution of *N*-acetyl-tryptophanamide (Figure 2(b) inset). In contrast, different spectra were obtained under native conditions (Figure 2(b)) suggesting that Trp located at surface-exposed locations can provide sensitive probes to monitor the folding/unfolding transition. Equilibrium-unfolding curves of each mutant were then monitored in order to determine that the stability of Ub is not altered by Trp insertion. All five curves (Figure 2(c)) fit well to a two-state model showing single transitions of similar steepness (similar *m*-value; see Table 1). The extrapolated free energies of unfolding in water (ΔG^{H2O}) were also found to be similar to the values obtained for wild-type Ub using NMR or CD to monitor unfolding (31 kJ mol^{-1}and 28.0 kJ mol^{-1}, respectively).[15]

We then assessed the unfolding kinetics of the different mutants using GdnHCl-jump experiments (Figure 3). All kinetic traces fit well to a single exponential function (Figure 3(a), left) and the amplitude of the transitions accounted well for the N→U fluorescence change expected at various denaturant concentrations (Figure 3(a), right). Unfolding rate constants of the different mutants fit well *versus* denaturant concentration to a two-state chevron curve model and were found to be similar within one order of magnitude (Figure 3(b)). Both the stabilities and *m*-value estimated from the chevron curve were found to be similar to values obtained in equilibrium experiments (Table 1). This suggests that no folding I-state is populated significantly during folding/unfolding of Ub above 2 M GdnHCl. The different mutants also displayed similar unfolding rate denaturant dependence. Their estimated β_T-values (Table 1), which provide a measure for the relative compactness of the transitions-state, were similar to that of Ub^{F45W} (0.69)

Table 1. Stabilities and *m*-values of Ub^{M1W}, Ub^{A28W}, Ub^{F45W}, Ub^{S57W}, and Ub^{T66W} obtained using equilibrium (e) folding (F) or unfolding (U) experiments or kinetic (k) unfolding experiments at 30 °C

	F/U	ΔG^{H_2O} [a]	m[b]	β_T[c]
Ub^{M1W}	F (e)	35.4 (5.2)	10.5 (1.6)	
	U (e)	26.8 (3.3)	8.3 (1.1)	
	U (k)	31.8 (1.4)	10.0 (0.5)	0.75 (0.06)
Ub^{A28W}	F (e)	35.2 (4.6)	10.8 (1.4)	
	U (e)	30.6 (1.5)	9.5 (0.5)	
	U (k)	29.1 (0.7)	8.7 (0.2)	0.73(0.05)
Ub^{F45W}	F (e)	27.1 (24)	8.8 (0.8)	
	U (e)	26.8 (1.1)	8.7 (0.4)	
	U (k)	30.3 (1.5)	10.1 (0.5)	0.69 (0.04)
Ub^{S57W}	F (e)	27.9 (1.7)	9.2 (0.5)	
	U (e)	34.3 (6.7)	11.0 (2.3)	
	U (k)	30.9 (1.6)	9.8 (0.5)	0.69 (0.03)
Ub^{T66W}	F (e)	27.0 (6.1)	9.4 (2.1)	
	U (e)	23.6 (2.5)	8.1 (1.0)	
	U (k)	28.6 (4.9)	9.5 (1.7)	0.66 (0.14)

[a] The free energies of folding (ΔG) are in units of kJ mol^{-1}. Kinetic ΔG (k) are determined from the folding and unfolding rate constants extrapolated in water from the chevron curve fits of the kinetic unfolding experiments: $\Delta G_k = RT \ln(k_{UN}/k_{NU})$.

[b] The *m*-values are in kJ mol^{-1} M^{-1}. Kinetic *m*-values (k) are the sum of the slope of the denaturant dependence for the unfolding and folding rates (m_{NU}–m_{UN}) multiplied by the factor *RT* (gas constant times temperature).

[c] The β_T-values are determined from $1 - m_{NU}/m_{e\ (F)}$.

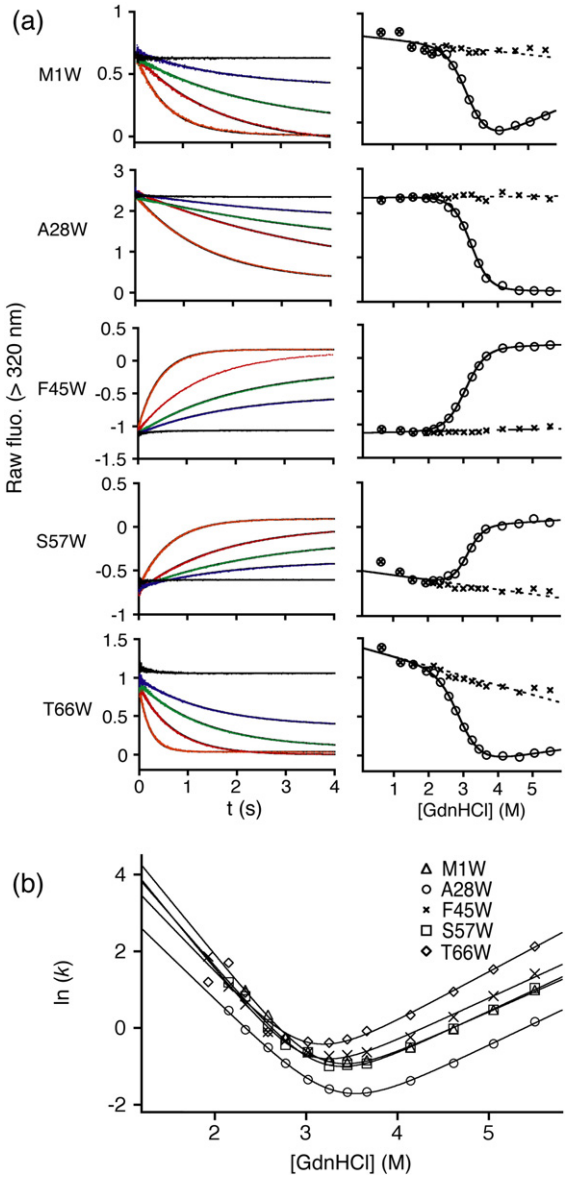

Figure 3. Unfolding kinetic characterization of the different single Trp mutants. (a) Left: unfolding kinetic traces of the different Trp mutants in 5.05 M (orange), 4.14 M (red), 3.45 M (green), 3.02 (blue) and 2.15 M GdnHCl fit to single-exponential functions. Right: fluorescence signal extrapolated at the initiation (crosses) and end-point (circles) of the kinetic unfolding trace fit well to the expected N-like signal (dotted line) and a two-state equilibrium curve, respectively. (b) Unfolding rate constants of the Trp mutants *versus* GdnHCl concentration fit to a two-state mechanism (chevron curve). See Table 1 for thermodynamic parameters extrapolated from the best fits.

(values near zero or 1 indicate a level of compaction similar to the U-state or the N-state, respectively).[3] These results suggest that above 2 M GdnHCl, the folding/unfolding transition-states of all mutants have similar compactness and that Trp insertions at solvent-exposed locations on the protein do not perturb the folding/unfolding mechanism significantly. To ensure that the different Trp insertions do not alter the folding landscape of Ub at low concentrations of denaturant, the folding kinetics of all mutants were also studied using ANS fluorescence as a probe (fluorescence quantum yield of this dye increases markedly when bound to exposed clusters of hydrophobic residues in partially folded proteins).[41] All mutants showed a comparable biphasic decrease of fluorescence during refolding in 0.45 M GdnHCl (Figure 4) and the rate constants of both transitions detected, k_{f1} and k_{f2}, were found to be similar to the rate constants of T_1 and T_2 (Table 2 and Figure 1). Taken together, these results suggest that Trp insertion at solvent-exposed positions has little impact on either the stability or the folding/unfolding landscape of Ub and provide sensitive and structure-specific probes to monitor its refolding.

The denaturant-dependent folding transition leads to a structurally distinct late I-state

We then assessed how the different Trp probes report Ub folding transitions (Figure 5). At low concentrations of denaturant, two exponential terms were sufficient to model the recovery of native-like fluorescence of all mutants between 3.2 ms and 300 ms of refolding time with the exception of Ub^{T66W}, which required only a single exponential (Figure 5(a) and (b); see Material and Methods for fitting procedure). The two folding transitions displayed rate constants similar to those obtained with ANS fluorescence: at 0.45 M GdnHCl, k_{f1} varied from 121 s^{-1} to 327 s^{-1} depending on the mutant (average value obtained with ANS, 134 s^{-1}), and k_{f2} varied from 11.5 s^{-1} to 17.5 s^{-1} (average value obtained with ANS, 19.9 s^{-1}) (Table 2). At low concentrations of denaturant, k_{f1} fit well to the expected two-state folding transition (Figure 5(c): open circles fit to black dotted line), and the denaturant dependence of k_{f2} was found to be relatively independent of the concentration of GdnHCl (open squares). The only folding transition detected with Trp66 displayed a rate constant and denaturant dependence similar to the second transition (13.9 s^{-1} in 0.45 M GdnHCl). Signs of apparent burst phase amplitude were detected at low concentrations of denaturant for Ub^{M1W}, Ub^{A28W} and Ub^{T66W}, since a discrepancy was observed between the fluorescence signal extrapolated to the initiation time of the folding reaction, F_0, and the linear extrapolation of the U-state fluorescence (dotted line; Figure 5(b)). This suggests that an additional folding transition could take place during the dead-time of the stopped-flow instrument.[20,42] Concerning the refolding amplitudes of the two detected transitions (A_1 and A_2), both were found to vary strongly depending on probe location. The majority of the expected refolding amplitude occurred during T_1 for Ub^{A28W} and Ub^{F45W} while most or all of the expected refolding amplitude was detected during T_2 for Ub^{S57W} and Ub^{T66W}, respectively (Table 2 and Figure 5(b)). Surprisingly, A_1 was opposite to that for the expected U→N transition for Ub^{S57W}. In contrast, the fluorescence signal of Ub^{M1W} increased during T_1 to a level that is twice the value of its N-state signal (Figure 5(b): F_1 *versus*

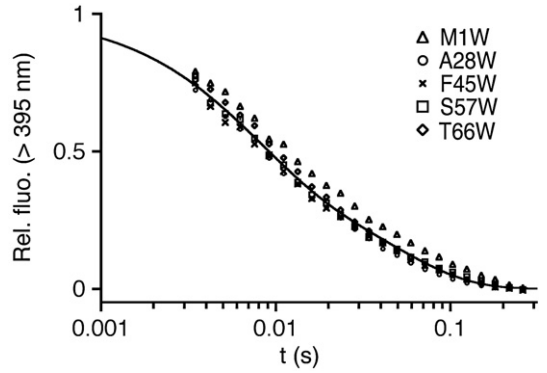

Figure 4. Folding kinetic traces of the different Trp mutants monitored using ANS fluorescence in 0.45 M GdnHCl (395 nm cut-off filter). All traces were well fit with the sum of two exponential functions. The line represents the fit obtained for the wild-type Ub refolding trace. Rate constants and amplitudes of the two transitions detected are reported in Table 2. Refolding traces contain fewer points in order to distinguish all mutants.

Table 2. Rate constants (k) and amplitudes (A) of the transitions detected during the refolding of Ub^{wt}, Ub^{M1W}, Ub^{A28W}, Ub^{F45W}, Ub^{S57W}, and Ub^{T66W} in 0.45 M GdnHCl using Trp or ANS as fluorescent probes

Probes		k_{f1}	k_{f2}	A_0	A_1	A_2	$A_{U\text{-}N}$
ANS	*wt*	146	21.0	–	0.58	0.42	1
	M1W	114	15.0	–	0.60	0.41	1
	A28W	156	25.0	–	0.57	0.43	1
	F45W	151	20.8	–	0.61	0.39	1
	S57W	128	17.7	–	0.66	0.34	1
	T66W	120	20.9	–	0.60	0.40	1
Trp	*wt*	–	–	–	–	–	–
	M1W	327	11.5	−0.56	−0.58	0.64	−0.50
	A28W	162	17.5	−0.40	−0.36	−0.08	−0.84
	F45W	178	15.6	0.11	0.75	0.20	1.06
	S57W	121	13.7	0.00	−0.08	0.65	0.57
	T66W	–	13.9	−0.40	–	−0.64	−1.04

The rate constant (s^{-1}) and refolding amplitudes of the two folding transitions detected during Ub refolding between 3.2 ms and 300 ms of refolding time in 0.45 M GdnHCl using ANS or Trp fluorescence as probes. k_{f1}, k_{f2}, A_1, and A_2 represents the rate constants and refolding amplitudes of T_1 and T_2, respectively. A_0 represents the difference in amplitude between the fluorescence signal extrapolated at the initiation time of refolding and the expected unfolded fluorescence signal (burst phase). $A_{U\text{-}N}$ represents the refolding amplitude expected for the U→N transitions, which was set to 1 in the case of the refolding traces monitored with ANS. The error is <10% for rate constants and <0.01 for the refolding amplitudes.

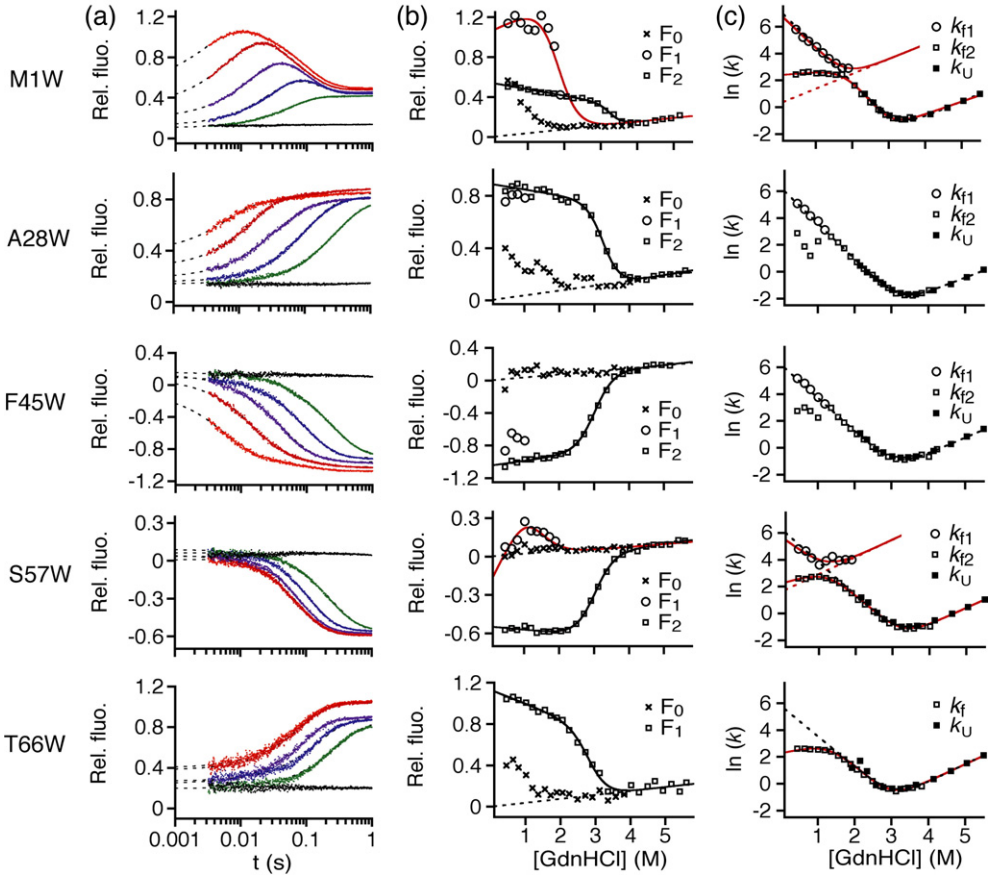

Figure 5. Folding kinetic characterization of the different single Trp mutants monitored using Trp fluorescence (320 nm cut-off filter). (a) Refolding traces obtained between 3.2 ms and 300 ms at various concentrations of GdnHCl (orange, 0.45 M; red, 0.80 M; purple, 1.19 M; blue, 1.55 M; green, 1.89 M; black, 4.02 M). (b) Fluorescence values extrapolated at the initiation of refolding (F_0), after T_1 (F_1), and after T_2 (F_2); F_2 fits well to a two-state folding model using the parameters obtained from the equilibrium experiment (black line). The red line corresponds to a two-state fit of F_1, the fluorescence signal obtained after T_1. The broken line corresponds to the linear extrapolation of the expected fluorescence of the U-state. Apparent burst phases can be detected by comparing F_0 with this latter value. (c) Rate constants of folding transitions T_1 and T_2 (k_{f1} and k_{f2}) together with the unfolding rate constant (k_U). The broken black line corresponds to a two-state chevron curve fit of k_f and k_U under the apparent two-state conditions ([GdnHCl]>2 M). Red lines correspond to the three-state on-pathway fit of the data (see Materials and Methods for the fitting procedure and Table 3 for parameters obtained from the best fits).

F_2) before decreasing to the native-like level during T_2. These refolding profiles obtained at a protein concentration of 15 μM at pH 7.0 were similar at different concentrations of protein (down to 1 μM) and at lower pH (5.0) (see the Supplementary Data). In summary, all Trp probes detected two transitions in Ub refolding (with the exception of Trp66, see the section Protein kinetic I-state highlighted using a combination of Trp probes, below), and T_1 and T_2 showed similar rates but very different relative amplitudes depending on the Trp position (Table 2).

Knowing that the different Trp mutations do not perturb the Ub folding landscape significantly, we compared the refolding amplitudes of T_1 and T_2 obtained with different Trp probes in order to assess the nature of these transitions (Figure 1). To begin with, the analysis of Ub^{S57W} demonstrates that T_1 cannot represent a direct path from U to N, since A_1 is inverted compared to the expected U→N fluorescence amplitude change ($A_{U\text{-}N}$) in the absence of an apparent burst phase (Table 2). This suggests that the denaturant-dependent folding transition of Ub does not lead the protein directly to the N-state but rather to a structurally distinct late I-state (U→I). The term late is used in order to distinguish the I-state formed during T_1 from the state that may be formed earlier within the dead-time of the stopped-flow instrument. The stability of this late I-state can be further inferred from the denaturant effect on both F_1, the fluorescence level obtained after T_1, and k_{f1}, the observed rate constant for the I-state formation (Figure 5(b) and (c): Ub^{S57W}). At concentrations above 1.5 M GdnHCl, F_1 decreases in a cooperative manner while k_{f1} displays an upward deviation. This suggests that the late I-state becomes less stable than the U-state at concentrations above 1.5 M GdnHCl and, therefore, no longer accumulates (k_{f1} increases is attributable to the enhancement of the I-state unfolding rate).

Evidence that T_2 represents the rate-limiting rearrangement of the late I-state into the N-state (I→N) is provided by the correlation observed between k_{f2} roll over at low concentrations of denaturant and the amount of I-state that accumulates after T_1. Specifically, as the late I-state becomes destabilized above 1.5 M GdnHCl, k_{f2} displays the characteristic of an apparent two-state transition (Figure 5(b) and (c): Ub^{S57W}). Similar observations are obtained from the analysis of Ub^{M1W}, with the exception that Trp 1 cannot distinguish T_1 from T_2 above the I-state mid-point of denaturation, because their amplitudes (A_1 and A_2) become of similar sign (the formation of less than half of the Ub^{M1W} I-state population displays a fluorescence amplitude that is smaller than the expected U→N transition), and k_{f1} and k_{f2} are too similar to be distinguished (within threefold). This limitation in probe efficiency becomes even more apparent and problematic in the case of Trp28 and Trp45, because these probes cannot even distinguish T_1 from T_2 above 1 M GdnHCl, since their amplitudes change in the same direction and rate constants are too similar. Interestingly, Trp66 represents an extreme case of probe inefficiency, since it is not sensitive to the formation of the late I-state (T_1). This suggests that Trp66 displays similar levels of fluorescence in both the U and I-states, U→I. Finally, no evidence of correlation is observed between the burst phase and the other transitions: k_{f1} does not deviate from linearity as the burst phase is enhanced in Ub^{M1W} or in Ub^{A28W}, and A_2 remains similar in Ub^{M1W} as the burst phase disappears around 1.5 M GdnHCl. These results add further evidence against the hypothesis that T_2 represents a parallel pathway in which a fraction of the protein slowly rearranges into the N-state after having been trapped in a slow folding I-state (burst phase) (see Figure 1). In the absence of any direct kinetic measurements, and without any evidence of kinetic coupling with either T_1 or T_2, the burst phase remains a subject for further research (see Discussion).

Protein kinetic I-state highlighted using a combination of Trp probes

As described in the previous section, only two of the five Trp probes studied (Trp1 and Trp57) were sensitive to the formation and rearrangement of the late I-state during Ub refolding. Trp28 and Trp45 displayed only small fluorescence changes during the I-state rearrangement into the N-state (T_2) and Trp66 did not detect the formation of the I-state (T_1). However, two Trp probes that display opposite fluorescence changes during T_1 and T_2 can be combined in the same mutant in order to confirm that the observed transitions represent the formation and rearrangement of a structurally distinct intermediate and not parallel folding pathways. For example, Trp45 fluorescence is quenched during the U→I transition, while Trp66 fluorescence is enhanced during the I→N transition (Figure 6(a), black dots). Therefore, the fluorescence of double

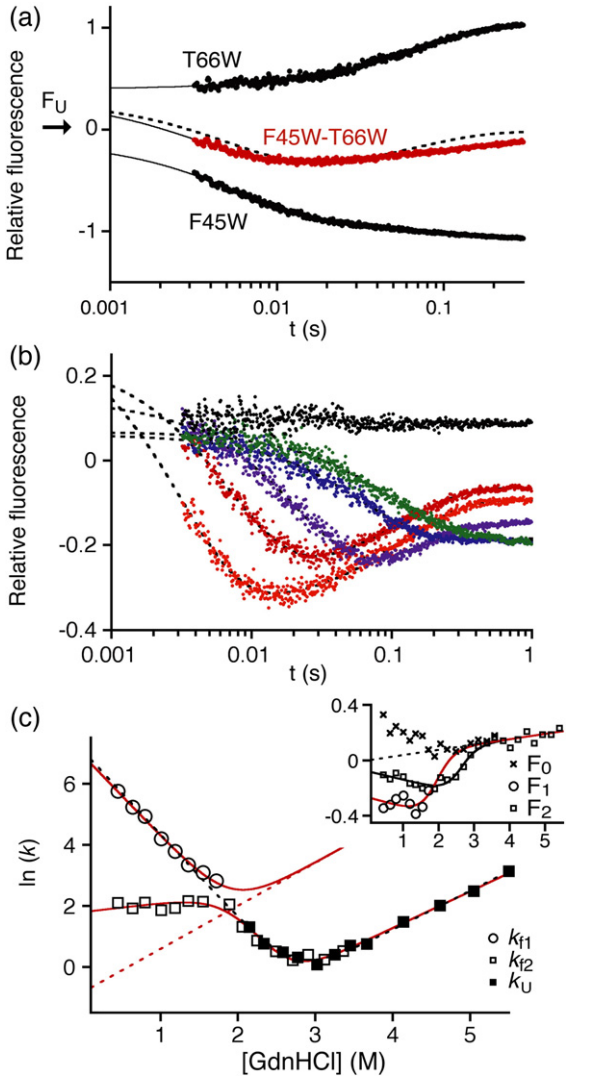

Figure 6. Folding kinetic characterization of the double Trp mutant $Ub^{F45W-T66W}$ monitored using Trp fluorescence (320 nm cut-off filter). (a) Refolding traces of single Trp mutants Ub^{F45W}, and Ub^{T66W} (black filled circles), and the predicted (dotted line) and experimentally determined (red filled circle) refolding traces of the double Trp mutant $Ub^{F45W-T66W}$. (b) Refolding traces of $Ub^{F45W-T66W}$ at various concentrations of GdnHCl (orange, 0.45 M; red, 0.80 M; purple, 1.19 M; blue, 1.55 M; green, 1.89 M; black, 4.02 M). (c) Rate constants of the folding and unfolding transitions. The broken black line corresponds to a two-state chevron curve fit of k_f and k_U in the apparent two-state conditions ([GdnHCl]> 2 M). Red lines correspond to a three-state on-pathway fit of the data (see Materials and Methods for the fitting procedure and Table 3 for parameters obtained from the best fit). Inset: fluorescence values extrapolated at the initiation of refolding (F_0), after T_1 (F_1), and after T_2 (F_2). F_2 fits well to a two-state unfolding model using the parameters obtained from the equilibrium experiment (black line). The red line corresponds to a two-state fit of F_1, the fluorescence signal obtain after T_1. The broken line corresponds to the linear extrapolation of the expected fluorescence of the U-state.

Trp mutant $Ub^{F45W-T66W}$ should provide an ideal probe to highlight the late I-state, since its fluorescence intensity is expected to decrease during the I-state formation (T_1), and increase during its rearrangement into the N-state (T_2) (see Figure 6(a), dotted line). We investigated the refolding of $Ub^{F45W-T66W}$ *versus* concentration of denaturant (Figure 6(b)) and found that the rates and amplitudes of both folding transitions were in close agreement with the values expected from combining Trp45 and Trp66 in the same protein (Figure 6(a), compare red filled circles with the black dotted line). In addition, adding Trp66 to Ub^{F45W}, or Trp45 to Ub^{T66W} also allowed us to clearly highlight the late I-state in the refolding of both Ub^{F45W}, and Ub^{T66W} since Trp66 alone could not detect the formation of the I-state, and Trp45 alone could hardly distinguish the late I-state from the N-state.

Global fitting analysis shows that the late I-state is compact, misfolded, and on-pathway

Having found that the denaturant-dependent transition does not represent a direct path from the U to N-states but rather the formation of a structurally distinct late I-state, we needed to confirm whether this alternative state is on or off-pathway. To do so, we simultaneously fit k_{f1}, k_{f2}, k_U and F_1, for mutants Ub^{M1W}, Ub^{S57W}, and $Ub^{F45W-T66W}$ to both on and off-pathway models over all concentrations of denaturant (see Materials and Methods for the fitting procedure). The similarity between the rates for formation (k_{f1}) and rearrangement (k_{f2}) of the I-state allowed us to distinguish between both mechanisms.[43] The kinetic data of all three mutants fit well to an on-pathway model (red lines in Figures 5(b) and (c), and 6(c)) and the best parameters obtained for the fits allowed for an estimate of the stabilities and the *m*-values of the different mutants (Table 3). On the other hand, the kinetic data obtained for Ub^{M1W} and $Ub^{F45W-T66W}$ could not be fit to an off-pathway mechanism, because the I-state unfolding rate (k_{IU}) could not be found equal to or higher than the I-state rearrangement rate into the N-state (k_{IN}) at low concentrations of denaturant (data not shown; see also Figure 7(b)).

The denaturant dependence of U_I (m_{UI}), F_1 (m_I), and k_{IN} (m_{IN}) obtained from the best fit also suggest that all three mutants display similar folding mechanism (Table 3). From the m_{UI}-values, we can estimate that the relative degree of compaction of the transition-state for the formation of the late I-state, β_{TS1}, lies between 0.53 and 0.59, depending on the Trp position. From the m_I-values, one can estimate that the compactness of the I-state, β_I, lies between 0.82 and 0.90. The stability of this I-state is also found to be relatively high: its average value being around half of the N-state stability (15.5 kJ mol^{-1}), although lower in the case of Ub^{S57W} (10.1 kJ mol^{-1}). Finally, the rate constants for the I→N transition of each mutant (k_{IN}) were all found to increase slightly with the concentration of denaturant (positive m_{IN}-values) suggesting that the second T-state is less compact than the I-state (β_{TS2}, 0.66–0.79). This suggests that the late I-state rearrangement proceeds through a partial unfolding event, since, on average, approximately 13% of the buried surface in the I-state must be re-exposed to the solvent before folding can proceed to the N-state. This necessary local unfolding event suggests that some regions of the Ub structure may be misfolded in the I-state.

Double-jump experiments on mutant Ub^{M1W} confirm that the I-state is on-pathway

To further characterize the late misfolded I-state, we took advantage of the fluorescence characteristics of Trp1 that displays a much higher fluorescence signal in the I-state than in either the U-or N-

Table 3. Folding and unfolding parameters obtained from a three-state on-pathway global fit analysis of k_{f1}, k_{f2}, k_U and F_1 for Ub^{M1W}, Ub^{S57W}, and $Ub^{F45W-T66W}$

		Thermodynamic parameters[a]				Kinetic parameters[b]			
Transitions→		U-N (e)	U-N[c] (k)	U-I[c] (k)		U→I	I→U	I→N	N→I
Ub^{M1W}	ΔG	35.4 (5.2)	33.6 (1.9)	16.8 (0.9)	k	1060	1.3	10.9	0.013
	m	10.5 (1.6)	11.1 (0.8)	9.3 (0.3)	m	−6.52	2.78	0.60	2.38
	β_T[d]	–	–	β_I (0.84)	β_T[d]	β_{TS1}=	0.59	β_{TS2}=	0.79
Ub^{S57W}	ΔG	27.9 (1.7)	30.4 (2.1)	10.1 (0.6)	k	284	5.15	9.5	0.003
	m	9.2 (0.5)	9.3 (1.7)	8.4 (0.7)	m	−5.16	3.24	2.25	3.13
	β_T[d]	–	–	β_I=0.90	β_T[d]	β_{TS1}=	0.56	β_{TS2}=	0.66
$Ub^{F45W-T66W}$	ΔG	24 (6)	32.9 (3.2)	19.5 (2.1)	k	1012	0.44	6.0	0.030
	m	10 (2)	12.4 (1.8)	10.2 (1.2)	m	−6.6	3.55	0.75	3.02
	β_T[d]	–	–	β_I=0.82	β_T[d]	β_{TS1}=	0.53	β_{TS2}=	0.76

[a] The free energies of unfolding in water (ΔG) are in units of kJ mol^{-1}. The *m*-values are in units of kJ mol^{-1} M^{-1}. (e) or (k) identify values that were determined from equilibrium (e) or kinetic (k) experiments, respectively.

[b] The rate constant (k) in water are in units of s^{-1}. Kinetic *m*-values are the slope of the denaturant dependence for the different transitions multiplied by the factor *RT* (gas constant times temperature).

[c] The thermodynamic parameters determined from the best fits of the kinetic data. ΔG_{UI}=–*RT* ln(k_{UI}/k_{IU}); ΔG_{UN}=–*RT* ln[(k_{UI} k_{IN})/(k_{IU} k_{NI})]; $m_I = m_{IU} - m_{UI}$; $m_k = m_{IU} - m_{UI} + m_{NI} - m_{IN}$.

[d] The β_T-value is the degree of compaction of a state or a transition-state relative to the U-state (0) and N-state (1) determined from the following ratio using m_k: $\beta_I = m_I/m_k$; $\beta_{TS1} = -m_{UI}/m_k$; $\beta_{TS2} = (m_I + m_{UI})/m_k$; where I, TS_1 and TS_2 represent the I-state and the transition states for the formation and rearrangement of the I-state, respectively.

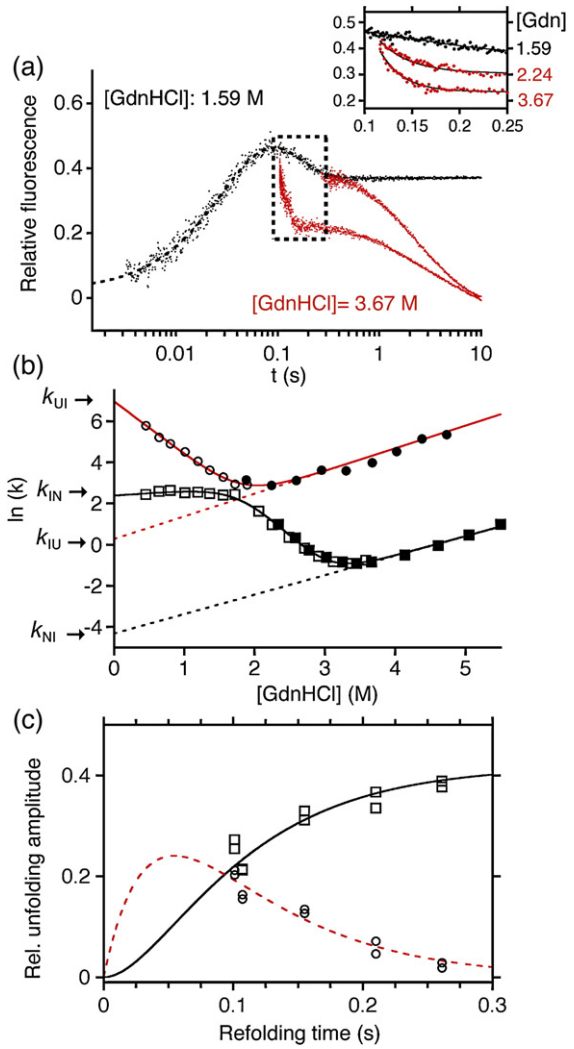

Figure 7. Characterization of Ub late I-state using folding/unfolding double-jump experiments on Ub^{M1W}. (a) Kinetic unfolding traces (red dots) obtained following a rapid jump in the concentration of GdnHCl (from 1.59 M to 3.76 M) after 101 ms (two unfolding transitions, 45 s^{-1} and 0.30 s^{-1}) and 261 ms of refolding (one unfolding transition, 0.35 s^{-1}, similar to the N-state unfolding rate constant). The concentration of GdnHCl used to refold Ub was selected in order to minimize the burst phase and allow sufficient kinetic resolution between T_1 and T_2. Inset: unfolding the I-state at different concentrations of GdnHCl; a magnification of (a). (b) Three-state modeling of the rate constants obtained from the folding/unfolding kinetic experiments on Ub^{M1W} (the fit is taken from Figure 5(c)). The unfolding rate constant of the late I-state obtained from the double-jump experiment (filled circles) fit perfectly with the predicted k_{IU} (red dotted line). (c) Kinetics of appearance or disappearance of both the I (circles) and N states (squares) *versus* folding time fit to an on-pathway sequential mechanism,[3] with the rate constant for formation and rearrangement of the I-state set to k_{f1} and k_{f2} (25 s^{-1} and 13 s^{-1}, respectively; $F_I = 2.2\ F_N$).

states. Rapid folding/unfolding double-jump experiments were performed on Ub^{M1W} in order to directly detect the late I-state unfolding transition (I→U) and therefore confirm the accuracy of the parameters obtained from the global fit analysis (Figure 7). After 101 ms of refolding time in 1.59 M GdnHCl (no burst phase observed at this concentration of GdnHCl), a rapid GdnHCl jump to 3.76 M showed two distinct Ub populations unfolding with rate constants of 45 s^{-1} and 0.30 s^{-1} (Figure 7(a), red dots). In contrast, after 261 ms of refolding, only the most stable protein population with an unfolding rate constant similar to the N-state (0.35 s^{-1}), remained detectable. The unfolding rate constant of the late I-state, k_{IU}, and its dependence on the concentration of denaturant were therefore directly determined using rapid unfolding jump experiments at various concentration of denaturant after 101 ms of refolding time in 1.59 M GdnHCl (Figure 7(a) inset). Both k_{IU} and m_{IU} were found to be identical with the values predicted by the global fitting analysis (Figure 7(b): filled circles fit to the red dotted line). Moreover, the on-pathway nature of the I-state can now be established directly, since the linear extrapolation of k_{IU} in water (red dotted line) is estimated to be around one order of magnitude slower than k_{IN}, the rate constant for the rearrangement of I-state into the N-state (1.3 s^{-1} *versus* 10.9 s^{-1}, respectively). In addition, the folding/unfolding double-jump experiment also demonstrates that T_1 and T_2 represent the sequential formation of two different species during Ub refolding (Figure 7(c)). First, the amplitude of the fastest unfolding transitions (circles), corresponding to the I-state population, could be well modeled *versus* refolding time by using k_{f1} and k_{f2}, the rate constant for the formation and rearrangement of the late I-state. Unfortunately, the rate of appearance of the late I-state could not be assessed directly due to the large dead-time associated with the double mixing experiments (101 ms). Also, the rate of formation of the N-state (squares, amplitude of the slowest unfolding transition *versus* refolding time) was similar to that of the disappearance of the I-state and was modeled accurately using an on-pathway three-state model using the same parameters.[3] Additional evidence in support of the sequential mechanism is suggested also by the fact that this modeling accounts correctly for all N-state formation (N-state population is extrapolated to zero at the initiation of refolding) implying that the entire N-state population originates from the rearrangement of the late I-state.

Discussion

One of the main advances provided by using several Trp probes to study protein refolding is that it allows discrimination between transitions that represent conformational changes that occur in the entire protein population *versus* those that correspond to parallel folding pathways (Figure 1). In the present study, the utilization of Trp1 and Trp57 allowed us to demonstrate for the first time that T_1 and T_2 do not represent parallel pathways, as suggested recently by Crespo *et al.*,[21] but rather the

formation and rearrangement of a late sequential I-state in a three-states mechanism (Figure 5). In addition, an appropriate combination of Trp probes (Trp45 and Trp66) allowed confirmation of the presence of this structurally distinct states (Figure 6). The advantage of selecting Trp probes that display large fluorescence changes to study a specific transition was also illustrated in the double-jump experiments when using the large fluorescence variation of Trp1 to detect the I→U transition (Figure 7). This specific probe allowed us to determine the stability, degree of compaction and on-pathway character of the I-state. Finally, the utilization of different single Trp probes also provided new indirect evidence suggesting that an early I-state may accumulate during the deadtime; Ub^{M1W}, Ub^{A28W} and Ub^{T66W} all displayed an apparent burst phase amplitude at low concentration of denaturant (Figure 5(b)) (see the section Ub may also refold through an early I-state below). In summary, our results describe how complex kinetic refolding reactions can be efficiently analyzed, first by using several Trp probes to detect and identify all relevant folding I-states, and then by characterizing each I or T-state using double-jump experiments (Figure 7). Further insights into the nature of I and T-states could be provided by Φ-value[3] or Ψ-value[44] analysis on specific Trp mutants that display the highest fluorescence sensitivity to a state or transition of interest. We believe that such an integrated strategy will provide a versatile approach to unambiguously characterize non-two-state protein folding mechanisms.

Folding mechanism of Ub

During the last decade, several groups have published more than 20 folding kinetic studies on Ub,[37] including both its complete Φ[24] and Ψ-value analysis.[23] In most of these works, Trp45 was the only fluorescence probe used to monitor Ub refolding and T_1, the major refolding transition detected, was considered to be the only significant folding transition.[17–19,23,24,45] In this study, we present direct kinetic evidence to suggest that this transition represents instead the formation of a misfolded I-state displaying around half of the stability of the N-state and up to 85% of its degree of compaction. On the basis of these results, a new mechanism for Ub folding is presented in the next section.

Ub folds *via* a late misfolded I-state

The energy and relative compactness of the different states and transition states detected during the refolding of Ub^{M1W} (Table 3) at various concentrations of GdnHCl are illustrated by Figure 8. In the absence of denaturant, the energy barrier between U and TS_1, $\Delta G_{U\text{-}TS1}$, is found to be significantly smaller than the energy barrier between the late I-state (I_L) and TS_2, $\Delta G_{I\text{-}TS2}$, allowing the late I-state to accumulate. On the other hand, as the concentration of GdnHCl is raised, the U-state becomes more

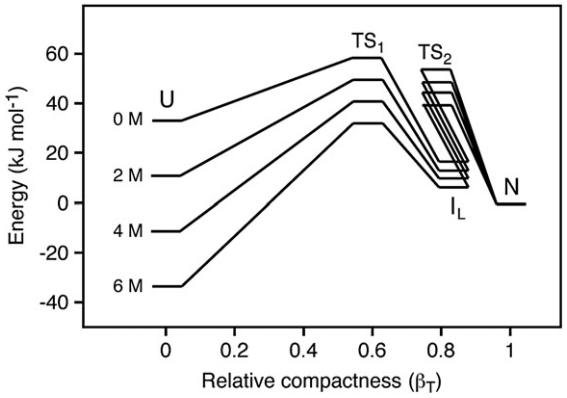

Figure 8. Free energy diagram for Ub folding/unfolding. The parameters obtained from Ub^{M1W} were used to calculate the free energies of the U, I, and the first and second transition states (TS_1 and TS_2) relative to the N-state at various concentrations of GdnHCl (see Table 3). A pre-exponential term of 2.4×10^7 s^{-1} was used to calculate the energy of the transition-states in this diagram. The *x*-axis reports the relative compactness of each species. The second transition-state (TS_2) of Ub is less compact than the late I-state (I_L), suggesting that some residues in the late I-state (I_L) have to be re-exposed to the solvent so that the polypeptide chain can reach the last transition state. Putative early folding I-states are not illustrated in this model.

stable relative to the other more compact states, and $\Delta G_{U\text{-}TS1}$ and $\Delta G_{I\text{-}TS2}$ become closer in height. If the Trp probe cannot efficiently distinguish the I-state from the N-state (e.g., Trp28 and Trp45), k_{IN} will be incorporated into k_{UI} as soon as the rate constants are found similar within threefold (~1 M GdnHCl); Ub will therefore display an apparent two-state mechanism (Figure 5(c)). As the concentration of GdnHCl is raised further (above 2 M GdnHCl for Ub^{M1W}), the I-state free energy will be increased above the U- and N-state free energies, and signs of the I-state will disappear from the refolding curves of all Trp mutants. In contrast, the late I-state could not be detected in conventional unfolding experiments, since $\Delta G_{I\text{-}TS1}$, the unfolding energy barrier for the I-state is smaller than $\Delta G_{N\text{-}TS2}$, the energy needed to unfold the N-state, at all concentrations of GdnHCl (Figure 8). Still, one of the most remarkable features of Ub late folding I-state is its high degree of compaction, even closer to the N-state than that of the last transition-state (β_I and β_{TS2} being 0.84 and 0.79, respectively, for Ub^{M1W}). This suggests that some buried residues in the late I-state have to be re-exposed to solvent so that the polypeptide chain can reach the last transition state. But what is the nature of this rearrangement, or what is causing such a large late rate barrier in Ub folding that is not found in other small, simple "two-state" folding proteins? A plausible hypothesis could be that some specific non-native interactions may prevent the misfolded I-state from rapidly accessing the N-state (specific energetic frustration[46,47]). In this case, $\Delta G_{I\text{-}TS2}$ would represent the energy that is needed to disrupt these interactions. Another possibility could be

that the complexity of the Ub fold requires the stepwise formation of a specific I-state in order to allow the protein to fold efficiently (topological frustration[48,49]). In this case, the misfolded I-state would be attributable to the complexity of the Ub fold rather than to specific non-obligatory detail of the sequence. Evidence from the literature would seem to support the latter hypothesis, as described below.

The most suggestive evidence concerning the nature of T_2 was likely reported in the first kinetic folding study on wild-type Ub using NMR and pulse deuterium/hydrogen exchange experiments to monitor amide H-bond formation *versus* refolding time.[50] In this pioneering work, Briggs and Roder noted that amide H-bonds of residues 59, 61, and 69 were protected at a slower rate (similar to k_{f2}) than the majority of the other residues, as Ub refolds in 1 M GdnHCl (25 °C, pH 5.0). This observation provided evidence for the subsequent stabilization or packing of the C-terminal segment (3_{10} helice and last β-strand).[50] This result is also consistent with the refolding amplitude obtained in the present study, since Trp57 and Trp66, both located in this specific region of the protein, displayed the highest fluorescence sensitivity to T_2.

Additional evidence in support of this model is found in a recent study by Searle *et al.*, who provide interesting data on a mutant in which the last C-terminal β-strand is destabilized.[21] In this study, the authors found that the mutant $Ub^{T66A\text{-}H68A}$ (two mutations at solvent-exposed residue positions) produced a ~20-fold acceleration in the N-state unfolding rate (from around 0.007 s^{-1} to 0.14 s^{-1} in water), which revealed another unfolding transition with a rate constant that is very similar to the unfolding rate constant of our late I-state (0.27 s^{-1} in water *versus* 0.44 s^{-1} in water for $Ub^{F45W\text{-}T66W}$ k_{IU}). Interestingly, the energy diagram presented in Figure 8 predicts that the unfolding transition of the Ub late I-state could be detected in single-jump unfolding experiments if a mutation would render $\Delta G_{N\text{-}TS2}$ similar to $\Delta G_{I\text{-}TS1}$. The double mutation T66A-H68A appears to have selectively destabilized the N-state but not the late I-state, suggesting that the last C-terminal segment of Ub is not yet found in its native-like β-strand conformation in the late I-state. Finally, it is important to mention that Φ- and Ψ-value analysis performed on Ub is not in contradiction with that of the present model, although no direct sign of late folding I-state was detected by fluorescence of Trp45 on any of the single-point mutants studied.[23,24,40] As we saw above, the absence of evidence for the I-state can be attributable to the fact that the U→I transition appears much similar to the U→N transition. Also, it is interesting to note that both Φ- and Ψ-value experiments have been conducted at lower temperature (25 °C[24] or 20 °C [23,40]) where temperature-insensitive k_{IN} may already be incorporated into k_{UI} [lowering the temperature selectively decreases k_{UI} relatively to k_{IN} (data not shown)]. Φ-value analysis finds that native-like interactions in the C-terminal part of Ub are not yet formed in the rate-limiting transition state;[23,24,40] indeed, the late rearrangement (k_{IN}) is probably not rate limiting at lower temperature. In apparent contrast, Ψ-value analysis performed at 2.0 M GdnHCl suggests that the last β-strand of Ub is in close proximity to its adjacent β-strands in the apparent "two-state" transition-state.[23,40] However, Ψ-value analysis cannot confirm whether this β-strand is properly packed into the core of Ub. Besides, one should expect that the apparent two-state transition detected in 2 M GdnHCl might be different from TS_1, since the I-state is destabilized around this concentration of denaturant. It will be interesting to compare how Φ- and Ψ-value analysis depicts TS_1, TS_2, and the late I-state when studying Ub refolding under the appropriate conditions (i.e., low denaturant concentration, higher temperature, or simply using the more efficient Trp1 or Trp45/Trp66 probes combination to monitor refolding) in order to see whether the presence of the late I-state could explain the apparent discrepancy observed between both approaches.[23,24,39,40]

In summary, the evidence presented above suggests that the late folding rearrangement of Ub may implicate the subsequent stabilization or packing of the C-terminal segment of the protein (3_{10} helix and last β-strand). On the other hand, these results do not indicate why this late rearrangement necessitates such a high rate barrier. Concerning this question, it is interesting to note that a late I-state has been detected during the refolding of GB1, a protein with topology similar to that of Ub but no amino acid identity[51] (see also debate on this I-state[6,20]). The degree of compaction of both the I-state and the last transition-state were also found to be similar to that of Ub (β_I and $\beta_{TS2} = 0.85$). *raf* RBD, a Ub superfold member, was found to fold *via* two transitions displaying rate constants and rate denaturant dependences similar to Ub.[18] The Φ-value analysis further suggests that the apparent "two-state" folding transition-state of *raf* RBD has a structure that is similar to the transition-state of Ub.[52] Such similarities in folding landscapes in the absence of sequence detail resemblance suggest that the particular fold complexity of Ub may be at the origin of both the late I-state and transition-state. With specific Trp probes that distinguish between both the U→I and I→N transitions, Φ or Ψ-value analysis will allow to determine whether they represent common features of the folding pathway of Ub superfamily members.

Ub may also refold through an early I-state

The strongest evidence in support of the presence of an earlier folding transition during Ub refolding has been provided recently by Roder and colleagues using a rapid mixing device.[20] In this study, two additional minor transitions have been detected during the first milliseconds of refolding of Ub^{F45W} (τ~150 μs and 1.8 ms). Further analyses are required to determine whether such kinetic complexities that take place on the 0.1–2 ms time-scale (within the dead-time

of our stopped-flow instrument) suggest the formation of early on-pathway intermediates or more or less specific collapse events. In the present study, two results provide further evidence for accumulation of early species within the dead-time of our stopped-flow instrument (<3.2 ms). First, the decrease in ANS fluorescence intensity observed as Ub refolds suggests the presence of an early collapse state, since a high level of fluorescence of this probe is generally observed only upon ANS binding to hydrophobic patches, which are unlikely to be found in completely unfolded proteins.[41] The apparent burst phase observed at a low concentration of denaturant with Trp probes located at position 1, 28, and 66 provides additional evidence. However, it is important to note that care must be taken when interpreting an apparent burst phase, since it has been demonstrated that the extrapolation of F_0 (the fluorescence signal at the beginning of the refolding experiment) can be affected when more than 50% of a transition is hidden in the dead-time of the mixing instrument (which is the case here for T_1 at the lowest concentration of GdnHCl).[17] Other studies have provided evidence supporting both the presence and the absence of accumulation of an early I-state during the refolding of Ub. For example, Crespo *et al.* found a consistent discrepancy between the equilibrium and kinetic stabilities and the *m*-values they obtained for many Ub mutants which they attribute to the presence of a rapidly forming I-state (mean values: m_e=10.6 (0.6) kJ mol^{-1} M^{-1}; m_k=8.5 (0.6) kJ mol^{-1} M^{-1}). On the other hand, our results do not corroborate this observation, since both the three-state and the two-state analyses (above 2 M GdnHCl) of our kinetic data correctly estimated our equilibrium parameters (see Tables 1 and 3). It has been proposed that some non-two-state behaviour detected during Ub refolding at a low concentration of denaturant could be attributable to aggregation.[19] However, in the present study, refolding curves of Ub^{M1W}, a Trp mutant displaying a high fluorescence sensitivity for all phases, displayed similar kinetic and burst phase amplitude at different concentrations of protein (down to 1 μM) or at lower pH (5.0) (see Supplementary Data). Finally, small-angle X-ray scattering measurements performed by Sosnick and colleagues showed no sign of a collapsed state upon rapid dilution of Ub U-state into 0.75 M GdnHCl at pH 7, 20 °C[53] and CD data obtained by Galdwin & Evans further suggested that there is not a substantial build-up of secondary structure during the dead time (0.55 GdnHCl at pH 8.5, 20 °C).[68] With the recent advances in rapid mixing devices,[54] our capacity to perform efficient double-jump experiments, or Φ or Ψ-value analysis on Ub fastest refolding transitions will be greatly enhanced using the Trp mutants that display the largest fluorescence change (burst phase) during the dead-time of our conventional stopped-flow instrument (Ub^{M1W}, Ub^{A28W}, Ub^{T66W}).

General implications of this study

It has long been recognized that obligatory on-pathway intermediates can be present in the refolding mechanism of apparent two-state folding proteins if the barrier for formation of the I-state is higher than that for its rearrangement to the N-state,[55,56] or if the I-state free energy is higher than the U or N-states.[57] Here, we have described another case where a three-state system displays the characteristics of a two-state mechanism: when the fluorescence signal, stability, and level of compaction of a late low-energy I-state is similar to that of the N-state (mutants Ub^{A28W} and Ub^{F45W}). Under these conditions, the U→I folding transition will appear much similar to the expected U→N folding transition if the fluorescence signal is used to monitor refolding. In addition, we have demonstrated that an apparent roll-over of the refolding rate constant at a low concentration of denaturant can represent the signature of a late I-state if the probe used is sensitive only to the I→N rearrangement (Trp66). These results illustrate why protein folding kinetics have to be monitored with multiple Trp probes in order to detect the accumulation of all low-energy I-states and to assess whether heterogeneity in folding traces or roll over of the rate constant at low concentrations of denaturant represent evidence for late I-states that would have been "missed" due to the limitations of using only a single fluorescent probe. More generally, it has been shown recently that more than 50% of the reported two-state folding proteins, either the wild-type protein or some variants, show folding or unfolding rate constant deviations that suggest the presence of a structurally similar late folding rate barrier (β_{TS2}~0.9).[58] Combined with the fact that many late I-states have been reported recently in the folding of different small proteins (e.g. Ub, Im7,[59] En-HD,[60] barnase,[61] Rd-apocyt b_{562},[62] the third domain of PDZ[63] and cytochrome *c*[12]), these results suggest that late I-states may well represent a common feature of protein folding.

Materials and Methods

Protein constructs and expression

The coding sequence of mammalian ubiquitin was fused to a His_6 tag at its N terminus, MHHHHHHG. It has been found that a His-tagged variant of Ub is not susceptible to transient aggregation.[19] Trp mutations and expression of the different Ub mutants were carried out as described.[18] His-tagged proteins were purified at high concentration (~600 μM) in denaturing (6 M Gdn) or native conditions using Ni-NTA resin (Qiagen) and eluted from the column with 25 mM acid acetic.

Data collection

All experiments were performed in 50 mM sodium phosphate buffer (pH 7.0)[64] at 30(±0.1) °C to allow for proper kinetic resolution between T_1 and T_2. Fluorescence

emission spectra were obtained using a Varian Cary Eclipse spectrophotometer and represent the average of three acquisitions (0.1 s sampling time) taken every 2 nm (bandwidth of 2.5 nm) with $\lambda_{ex}=281$ nm. All folding/unfolding data are the average of three experiments acquired using an Applied Photophysics SX18.MV stopped-flow fluorimeter with $\lambda_{ex}=281$ nm (2.5 nm bandwidth) by reading fluorescence intensity using a 320 nm cut-off filter ($\lambda_{ex}=350$ nm using a 395 nm cut-off in ANS experiments). Equilibrium stability curves were generated using the equilibrium end-point data of 10 s folding (Figure 2) or unfolding kinetic traces (Figure 3). Single-jump experiments were carried out by 1:10 mixing of denatured or native proteins (5.0 M and 1.0 M GdnHCl, respectively) with different concentrations of GdnHCl. Double-jump experiments were carried out by refolding denatured protein (5.0 M GdnHCl) with a sixfold dilution followed by a second mixing (2:5) with a different concentration of GdnHCl. The final concentration of GdnHCl in each experiment was determined by refractive index measurements with an Abbe 60 refractometer (Bellingham and Stanley Ltd) using an independent set of standard dilutions. The final concentrations of protein in single or double-jump experiments were ~15 μM and ~5 μM, respectively.[65] A concentration of 200 μM ANS was used in order to monitor the refolding of ~15 μM Ub molecules.

Data analysis

Data analysis was performed using the non-linear regression analysis program in Kaleidagraph (version 3.6 Synergy Software, pCS Inc.). Equilibrium data were fit to a two-state model assuming that the fluorescence intensity of the N and U-states, and $\Delta G_{U\text{-}N}$ are linear functions of the concentration of Gdn-HCl.[3] Proper adjustment of the time axis of the single and double mixing kinetic data set was obtained by performing an independent dead-time calibration of the stopped-flow instrument using *N*-bromosuccinimide quenching of *N*-acetyl-tryptophanamide fluorescence.[66] 0.7 ms (single mixing) and 2 ms (double mixing) were added to the *x*-axis and experimental data acquired before 3.2 ms (single mixing) and 3.5 ms (double mixing) were removed. The accurate minimal ageing time of the double-jump experiment (101 ms) was determined by comparing refolding traces of Ub^{M1W} obtained with both single and double mixing mode. Unfolding kinetic traces could be well described by a single-exponential function in the single-jump experiments. Refolding kinetic traces at low concentrations of denaturant were fit with two exponential terms between 3.2 ms and 300 ms. We use this time window that focuses on the first two phases and not the whole time-course in order to improve the fitting procedure. This allowed us to capture the complete N-like fluorescence recovery while getting rid of the additional minor folding transitions that always displayed small amplitude with all Trp probes (T_3 and T_4, not shown[18]). All the refolding and unfolding traces obtained for each Trp mutants were set relative to the fluorescence of the unfolded-state (between 2 M and 6 M GdnHCl), which was set to zero in the absence of GdnHCl (unless specified (Figure 3(a))). Unfolding rate constants (k_U) obtained in concentrations of GdnHCl above 2 M (Figure 3(b)) were fit to a classic two-state chevron curve.[3] Folding kinetic parameters of both the I and N-states were obtained from the best simultaneous fit of k_{f1}, k_{f2}, k_U, and F_1 over all concentrations of denaturant. The observed rate constant for formation of the I-state, k_{f1}, was fit to a chevron curve thus providing information on k_{UI}, k_{IU} , m_{UI}, and m_{IU} (and m_I and ΔG_{UI}, indirectly). The fluorescence obtained after T_1, F_1, was fit to a standard two-state equilibrium curve in order to obtain an estimate of m_I and ΔG_{UI}. Finally, k_{f2} and k_U, the observed rate for formation and unfolding of the N-state, respectively, were fit to a three-state on or off-pathway mechanism in order to obtain k_{IN}, k_{NI}, m_I and ΔG_{UI}.[67] Standard deviations were obtained from the best fit of the data.

Acknowledgements

The authors acknowledge F.X. Campbell-Valois, Tobin Sosnick and Sheena Radford for helpful discussions, Emily Manderson for critical reading of the manuscript, Mireille Fyfe for sequencing, and Jeffrey W. Keillor for providing access to the stopped-flow instrument. This work was supported by the NSERC of Canada (grant 194582-00). S.W.M. holds the Canada Research Chair in Integrative Genomics.

Supplementary Data

Supplementary data associated with this article can be found, in the online version, at doi:10.1016/j.jmb.2007.09.018

References

1. Plaxco, K. W., Simons, K. T. & Baker, D. (1998). Contact order, transition state placement and the refolding rates of single domain proteins. *J. Mol. Biol.* **277**, 985–994.
2. Jackson, S. E. (1998). How do small single-domain proteins fold? *Fold. De.* **3**, R81–R91.
3. Fersht, A. R. (1999). *Structure and Mechanism in Protein Science: A Guide to Enzyme Catalysis and Protein Folding*. W.H. Freeman, New-York.
4. Zarrine-Afsar, A., Larson, S. M. & Davidson, A. R. (2005). The family feud: do proteins with similar structures fold via the same pathway? *Curr. Opin. Struct. Biol.* **15**, 42–49.
5. Paci, E., Lindorff-Larsen, K., Dobson, C. M., Karplus, M. & Vendruscolo, M. (2005). Transition state contact orders correlate with protein folding rates. *J. Mol. Biol.* **352**, 495–500.
6. Krantz, B. A., Mayne, L., Rumbley, J., Englander, S. W. & Sosnick, T. R. (2002). Fast and slow intermediate accumulation and the initial barrier mechanism in protein folding. *J. Mol. Biol.* **324**, 359–371.
7. Brandts, J. F., Halvorson, H. R. & Brennan, M. (1975). Consideration of the Possibility that the slow step in protein denaturation reactions is due to cis-trans isomerism of proline residues. *Biochemistry*, **14**, 4953–4963.
8. Pappenberger, G., Aygun, H., Engels, J. W., Reimer, U., Fischer, G. & Kiefhaber, T. (2001). Nonprolyl cis peptide bonds in unfolded proteins cause complex folding kinetics. *Nature Struct. Biol.* **8**, 452–458.
9. Silow, M. & Oliveberg, M. (1997). Transient aggregates in protein folding are easily mistaken for folding intermediates. *Proc. Natl Acad. Sci. USA*, **94**, 6084–6086.

10. Wildegger, G. & Kiefhaber, T. (1997). Three-state model for lysozyme folding: triangular folding mechanism with an energetically trapped intermediate. *J. Mol. Biol.* **270**, 294–304.
11. Gianni, S., Travaglini-Allocatelli, C., Cutruzzola, F., Brunori, M., Shastry, M. C. & Roder, H. (2003). Parallel pathways in cytochrome *c*(551) folding. *J. Mol. Biol.* **330**, 1145–1152.
12. Krishna, M. M., Lin, Y. & Englander, S. W. (2004). Protein misfolding: optional barriers, misfolded intermediates, and pathway heterogeneity. *J. Mol. Biol.* **343**, 1095–1109.
13. Kim, P. S. & Baldwin, R. L. (1982). Specific intermediates in the folding reactions of small proteins and the mechanism of protein folding. *Annu. Rev. Biochem.* **51**, 459–489.
14. Wallace, L. A. & Matthews, C. R. (2002). Sequential vs. parallel protein-folding mechanisms: experimental tests for complex folding reactions. *Biophys. Chem.* **101–102**, 113–131.
15. Khorasanizadeh, S., Peters, I. D., Butt, T. R. & Roder, H. (1993). Folding and stability of a tryptophan-containing mutant of ubiquitin. *Biochemistry*, **32**, 7054–7063.
16. Khorasanizadeh, S., Peters, I. D. & Roder, H. (1996). Evidence for a three-state model of protein folding from kinetic analysis of ubiquitin variants with altered core residues. *Nature Struct. Biol.* **3**, 193–205.
17. Krantz, B. A. & Sosnick, T. R. (2000). Distinguishing between two-state and three-state models for ubiquitin folding. *Biochemistry*, **39**, 11696–11701.
18. Vallee-Belisle, A., Turcotte, J. F. & Michnick, S. W. (2004). raf RBD and ubiquitin proteins share similar folds, folding rates and mechanisms despite having unrelated amino acid sequences. *Biochemistry*, **43**, 8447–8458.
19. Went, H. M., Benitez-Cardoza, C. G. & Jackson, S. E. (2004). Is an intermediate state populated on the folding pathway of ubiquitin? *FEBS Letters*, **567**, 333–338.
20. Roder, H., Maki, K. & Cheng, H. (2006). Early events in protein folding explored by rapid mixing methods. *Chem. Rev.* **106**, 1836–1861.
21. Crespo, M. D., Simpson, E. R. & Searle, M. S. (2006). Population of on-pathway intermediates in the folding of ubiquitin. *J. Mol. Biol.* **360**, 1053–1066.
22. Roder, H. & Colon, W. (1997). Kinetic role of early intermediates in protein folding. *Curr. Opin. Struct. Biol.* **7**, 15–28.
23. Krantz, B. A., Dothager, R. S. & Sosnick, T. R. (2004). Discerning the structure and energy of multiple transition states in protein folding using psi-analysis. *J. Mol. Biol.* **337**, 463–475.
24. Went, H. M. & Jackson, S. E. (2005). Ubiquitin folds through a highly polarized transition state. *Protein Eng. Des. Sel.* **18**, 229–237.
25. Engelhard, M. & Evans, P. A. (1995). Kinetics of interaction of partially folded proteins with a hydrophobic dye: evidence that molten globule character is maximal in early folding intermediates. *Protein Sci.* **4**, 1553–1562.
26. Englander, S. W. & Kallenbach, N. R. (1983). Hydrogen exchange and structural dynamics of proteins and nucleic acids. *Quart. Rev. Biophys.* **16**, 521–655.
27. Englander, S. W., Sosnick, T. R., Englander, J. J. & Mayne, L. (1996). Mechanisms and uses of hydrogen exchange. *Curr. Opin. Struct. Biol.* **6**, 18–23.
28. Udgaonkar, J. B. & Baldwin, R. L. (1988). NMR evidence for an early framework intermediate on the folding pathway of ribonuclease A. *Nature*, **335**, 694–699.
29. Roder, H., Elove, G. A. & Englander, S. W. (1988). Structural characterization of folding intermediates in cytochrome c by H-exchange labelling and proton NMR. *Nature*, **335**, 700–704.
30. Korzhnev, D. M., Salvatella, X., Vendruscolo, M., Di Nardo, A. A., Davidson, A. R., Dobson, C. M. & Kay, L. E. (2004). Low-populated folding intermediates of Fyn SH3 characterized by relaxation dispersion NMR. *Nature*, **430**, 586–590.
31. Garvey, E. P., Swank, J. & Matthews, C. R. (1989). A hydrophobic cluster forms early in the folding of dihydrofolate reductase. *Proteins: Struct. Funct. Genet.* **6**, 259–266.
32. Smith, C. J., Clarke, A. R., Chia, W. N., Irons, L. I., Atkinson, T. & Holbrook, J. J. (1991). Detection and characterization of intermediates in the folding of large proteins by the use of genetically inserted tryptophan probes. *Biochemistry*, **30**, 1028–1036.
33. Mann, C. J., Royer, C. A. & Matthews, C. R. (1993). Tryptophan replacements in the trp aporepressor from Escherichia coli: probing the equilibrium and kinetic folding models. *Protein Sci.* **2**, 1853–1861.
34. Sherman, M. A., Beechem, J. M. & Mas, M. T. (1995). Probing intradomain and interdomain conformational changes during equilibrium unfolding of phosphoglycerate kinase: fluorescence and circular dichroism study of tryptophan mutants. *Biochemistry*, **34**, 13934–13942.
35. Steer, B. A. & Merrill, A. R. (1995). Guanidine hydrochloride-induced denaturation of the colicin E1 channel peptide: unfolding of local segments using genetically substituted tryptophan residues. *Biochemistry*, **34**, 7225–7233.
36. Azuaga, A. I., Canet, D., Smeenk, G., Berends, R., Titgemeijer, F., Duurkens, R. *et al.* (2003). Characterization of single-tryptophan mutants of histidine-containing phosphocarrier protein: evidence for local rearrangements during folding from high concentrations of denaturant. *Biochemistry*, **42**, 4883–4895.
37. Jackson, S. E. (2006). Ubiquitin: a small protein folding paradigm. *Org. Biomol. Chem.* **4**, 1845–1853.
38. Ramage, R., Green, J., Muir, T. W., Ogunjobi, O. M., Love, S. & Shaw, K. (1994). Synthetic, structural and biological studies of the ubiquitin system: the total chemical synthesis of ubiquitin. *Biochem J.* **299**, 151–158.
39. Fersht, A. R. (2004). Phi value versus psi analysis. *Proc. Natl Acad. Sci. USA*, **101**, 17327–17328.
40. Sosnick, T. R., Dothager, R. S. & Krantz, B. A. (2004). Differences in the folding transition state of ubiquitin indicated by phi and psi analyses. *Proc. Natl Acad. Sci. USA*, **101**, 17377–17382.
41. Semisotnov, G. V., Rodionova, N. A., Razgulyaev, O. I., Uversky, V. N., Gripas, A. F. & Gilmanshin, R. I. (1991). Study of the "molten globule" intermediate state in protein folding by a hydrophobic fluorescent probe. *Biopolymers*, **31**, 119–128.
42. Myers, J. K. & Oas, T. G. (2002). Mechanism of fast protein folding. *Annu. Rev. Biochem.* **71**, 783–815.
43. Heidary, D. K., O'Neill, J. C., Jr, Roy, M. & Jennings, P. A. (2000). An essential intermediate in the folding of dihydrofolate reductase. *Proc. Natl Acad. Sci. USA*, **97**, 5866–5870.
44. Sosnick, T. R., Krantz, B. A., Dothager, R. S. & Baxa, M. (2006). Characterizing the protein folding transition state using psi analysis. *Chem. Rev.* **106**, 1862–1876.
45. Platt, G. W., Simpson, S. A., Layfield, R. & Searle, M. S. (2003). Stability and folding kinetics of a ubiquitin mutant with a strong propensity for nonnative

beta-hairpin conformation in the unfolded state. *Biochemistry*, **42**, 13762–13771.
46. Bryngelson, J. D. & Wolynes, P. G. (1987). Spin glasses and the statistical mechanics of protein folding. *Proc. Natl Acad. Sci. USA*, **84**, 7524–7528.
47. Goldstein, R. A., Luthey-Schulten, Z. A. & Wolynes, P. G. (1992). Protein tertiary structure recognition using optimized Hamiltonians with local interactions. *Proc. Natl Acad. Sci. USA*, **89**, 9029–9033.
48. Shea, J. E., Onuchic, J. N. & Brooks, C. L., 3rd (1999). Exploring the origins of topological frustration: design of a minimally frustrated model of fragment B of protein A. *Proc. Natl Acad. Sci. USA*, **96**, 12512–12517.
49. Clementi, C., Nymeyer, H. & Onuchic, J. N. (2000). Topological and energetic factors: what determines the structural details of the transition state ensemble and "en-route" intermediates for protein folding? An investigation for small globular proteins. *J. Mol. Biol.* **298**, 937–953.
50. Briggs, M. S. & Roder, H. (1992). Early hydrogen-bonding events in the folding reaction of ubiquitin. *Proc. Natl Acad. Sci. USA*, **89**, 2017–2021.
51. Park, S. H., Shastry, M. C. & Roder, H. (1999). Folding dynamics of the B1 domain of protein G explored by ultrarapid mixing. *Nature Struct. Biol.* **6**, 943–947.
52. Campbell-Valois, F. X. & Michnick, S. W. (2007). The transition state of the ras binding domain of Raf is structurally polarized based on Phi-values but is energetically diffuse. *J. Mol. Biol.* **365**, 1559–1577.
53. Jacob, J., Krantz, B., Dothager, R. S., Thiyagarajan, P. & Sosnick, T. R. (2004). Early collapse is not an obligate step in protein folding. *J. Mol. Biol.* **338**, 369–382.
54. Roder, H., Maki, K., Cheng, H. & Shastry, M. C. (2004). Rapid mixing methods for exploring the kinetics of protein folding. *Methods*, **34**, 15–27.
55. Porschke, D. & Eigen, M. (1971). Co-operative non-enzymic base recognition. 3. Kinetics of the helix-coil transition of the oligoribouridylic-oligoriboadenylic acid system and of oligoriboadenylic acid alone at acidic pH. *J. Mol. Biol.* **62**, 361–381.
56. Tsong, T. Y. & Baldwin, R. L. (1972). A sequential model of nucleation-dependent protein folding: kinetic studies of ribonuclease A. *J. Mol. Biol.* **63**, 453–469.
57. Tanford, C. (1970). Protein denaturation. C. Theoretical models for the mechanism of denaturation. *Advan. Protein Chem.* **24**, 1–95.
58. Sanchez, I. E. & Kiefhaber, T. (2003). Evidence for sequential barriers and obligatory intermediates in apparent two-state protein folding. *J. Mol. Biol.* **325**, 367–376.
59. Capaldi, A. P., Kleanthous, C. & Radford, S. E. (2002). Im7 folding mechanism: misfolding on a path to the native state. *Nature Struct. Biol.* **9**, 209–216.
60. Mayor, U., Guydosh, N. R., Johnson, C. M., Grossmann, J. G., Sato, S., Jas, G. S. *et al.* (2003). The complete folding pathway of a protein from nanoseconds to microseconds. *Nature*, **421**, 863–867.
61. Vu, N. D., Feng, H. & Bai, Y. (2004). The folding pathway of barnase: the rate-limiting transition state and a hidden intermediate under native conditions. *Biochemistry*, **43**, 3346–3356.
62. Chu, R., Pei, W., Takei, J. & Bai, Y. (2002). Relationship between the native-state hydrogen exchange and folding pathways of a four-helix bundle protein. *Biochemistry*, **41**, 7998–8003.
63. Feng, H., Vu, N. D. & Bai, Y. (2005). Detection of a hidden folding intermediate of the third domain of PDZ. *J. Mol. Biol.* **346**, 345–353.
64. Maxwell, K. L., Wildes, D., Zarrine-Afsar, A., De Los Rios, M. A., Brown, A. G., Friel, C. T. *et al.* (2005). Protein folding: defining a "standard" set of experimental conditions and a preliminary kinetic data set of two-state proteins. *Protein Sci.* **14**, 602–616.
65. Pace, C. N., Vajdos, F., Fee, L., Grimsley, G. & Gray, T. (1995). How to measure and predict the molar absorption coefficient of a protein. *Protein Sci.* **4**, 2411–2423.
66. Peterman, B. F. (1979). Measurement of the dead time of a fluorescence stopped-flow instrument. *Anal. Biochem.* **93**, 442–444.
67. Bofill, R., Simpson, E. R., Platt, G. W. & Searle, M. S. (2005). Extending the folding nucleus of ubiquitin with an independently folding beta-hairpin finger: hurdles to rapid folding arising from the stabilisation of local interactions. *J. Mol. Biol.* **349**, 205–221.
68. Gladwin, B. F. & Evans, P. A. (1996). Structure of very early protein folding intermediates: new insights through a variant of hydrogen exchange labelling. *Fold Des.* **1**, 407–417.